frontiers in Ecology and Evolution

ORIGINAL RESEARCH
published: 23 September 2021
doi: 10.3389/fevo.2021.678186

Soil Macropores Affect the Plant Biomass of Alpine Grassland on the Northeastern Tibetan Plateau

*Ying Zheng[1,2], Ning Chen[1,2], Can-kun Zhang[1,2], Xiao-xue Dong[1,2] and Chang-ming Zhao[1,2]**

[1] State Key Laboratory of Grassland Agro-ecosystems, School of Life Sciences, Lanzhou University, Lanzhou, China,
[2] Yuzhong Mountain Ecosystem Field Observation and Research Station, Lanzhou University, Lanzhou, China

Macropores are an important part of soil structure. However, in alpine regions, the effects of soil macropores on soil properties and vegetation growth are not clear. We used the X-ray computed tomography (CT) method to obtain 3D images and visualize the distribution and morphology of soil macropores. By combining principal component analysis (PCA) and stepwise regression methods, we studied the relationships between soil macropores and both soil properties and vegetation growth in three types of grassland [alpine degraded steppe (ADS), alpine typical steppe (ATS), and alpine meadow steppe (AMS)] on the Tibetan Plateau. More tubular and continuous macropores occurred in the soil profiles of the AMS and ATS than in that of the ADS. In addition, the AMS soil had the highest macropore number (925 ± 189), while the ADS soil had the lowest macropore number (537 ± 137). PCA and correlation analysis suggested that macroporosity (MP) has significant positive correlations with the contents of soil organic matter, total nitrogen (TN), available phosphorus (AP) and total phosphorus (TP) ($p < 0.05$). The two parameters with the greatest influence on aboveground and belowground biomass were the shape factor ($p < 0.05$) and MP ($p < 0.05$), respectively. However, there was no significant correlation between plant diversity and soil macropores. We conclude that the irregularity of soil macropores restricts the growth space of roots and causes plants to sacrifice the accumulation of aboveground biomass for that of roots to find suitable sites for nutrient and water absorption.

Keywords: soil macropore, biomass, plant diversity, alpine stony soil, X-ray CT

OPEN ACCESS

Edited by:
Yun Jäschke, Senckenberg Museum of Natural History Görlitz, Germany

Reviewed by:
Zhongming Wen, Northwest A&F University, China
Minghua Song, Chinese Academy of Sciences (CAS), China

***Correspondence:**
Chang-ming Zhao
zhaochm@lzu.edu.cn

Specialty section:
This article was submitted to Conservation and Restoration Ecology, a section of the journal Frontiers in Ecology and Evolution

Received: *18 March 2021*
Accepted: *16 August 2021*
Published: *23 September 2021*

Citation:
Zheng Y, Chen N, Zhang C-k, Dong X-x and Zhao C-m (2021) Soil Macropores Affect the Plant Biomass of Alpine Grassland on the Northeastern Tibetan Plateau. Front. Ecol. Evol. 9:678186. doi: 10.3389/fevo.2021.678186

INTRODUCTION

Soil structure can regulate biophysical and chemical processes and properties in soil that are associated with soil function and plant growth, such as water retention and infiltration, gas exchange, soil organic matter and nutrient dynamics, root penetration and sensitivity to erosion (Bronick and Lal, 2005; Guimarães et al., 2017; Rabot et al., 2018). Soil structure and its effects on soil function deserve further research because soil structure affects soil water dynamics and nutrient cycling and thus is of great significance for understanding the relationship between soil and plant growth (Kuka et al., 2013). The term soil structure refers to the spatial arrangement of solids and voids across different scales without considering the chemical heterogeneity of the solid phase (Rabot et al., 2018). From the pore perspective, the soil structure is defined as the combination of different types of pores, where the surfaces of soil particles are assumed to be

the pore wall (Pierret et al., 2002; Jarvis, 2007; Colombi et al., 2017; Rabot et al., 2018). According to pore size, pores are generally divided into macropores, mesopores and micropores. Due to inconsistent classification criteria for macropores, the definitions of the equivalent pore size of macropores are somewhat vague in the literature, with some being greater than 1 mm and some greater than 3 mm (Iversen et al., 2012), although macropores are usually defined as pores having an equivalent diameter greater than 0.5 mm (Hlaváčiková et al., 2019).

Macropores are free spaces in the soil, and they form through plant root decay, soil faunal and microorganism activities, erosive processes and wetting and drying of the soil (Beven and Germann, 2013). Macropores are not only physically but also chemically and microbiologically different from the soil and may be rich in pathogenic or symbiotic microorganisms or depleted in nutrients (Passioura, 1991). In structural soils, macropore flow is the main process underlying priority flow; moreover, preferential flow pathways are considered biological hotspots, with a concentration of active microbial biomass (Jarvis, 2007, Jarvis et al., 2016; Zwartendijk et al., 2017; Fuhrmann et al., 2019). Beven and Germann (2013) suggested that during extreme rainfall, water flow is dominated by macropores, with the remaining pores being either dry or reached by only a small amount of water. Soil with macropores is highly aerated, and the body mucous of soil animals such as earthworms easily attaches to macropore walls; thus, the macropores represent a potential nutrient-rich area for plants (Kuka et al., 2013; Kautz et al., 2013, 2014).

In addition, macropores can affect root growth into the subsoil and allow the root system to pass through otherwise impermeable soils and access a larger pool of water and mobile nutrients (Hodge et al., 2009). Soil macropores play important roles in plant growth; in the subsoil, plant roots preferentially grow in macropores, which may have been formed by worms or by the roots of previous plants (biopores) or by gross movement of the soil to form slickensides and similar fissures (Hamblin and Hamblin, 1985; Athmann et al., 2013; Han et al., 2015). Regardless of the additional nutrient incentives of the macropore linings, root growth along macropores can improve plant access to subsoil areas with sufficient nutrient resources (Bauke et al., 2017; Landl et al., 2017). The effects of macropores on the hydrological process and nutrient cycle remain unclear, although it has been proposed that macropores represent hotspots of hydrological processes and nutrient cycles related to vegetation growth in alpine soil (Hu et al., 2020; Maier et al., 2020).

The Tibetan Plateau is characterized by low temperatures, dryness, ultraviolet radiation, freeze and thaw cycles and a short growing season, and the alpine grassland on the plateau is one of the most sensitive and vulnerable ecosystems to regional climate change and human activities (Xu et al., 2010). The soil structures under alpine vegetation can differ from those in non-alpine areas that contain fewer rock fragments (Gao et al., 2020); alpine grassland soil exhibits obvious stony characteristics, and the soil macropore size is different from that in non-alpine areas (Wang et al., 2011; Qin et al., 2015). Therefore, the vegetation in alpine areas grows under unique soil conditions and harsh climate conditions.

Due to differences in water and temperature conditions, soil animals, plants, etc., different grassland types vary in their influences on soil pore structure (Hu et al., 2016, 2020; Gao et al., 2020; Meurer et al., 2020); however, the effects of different soil macropore structures on soil properties and vegetation growth are not yet clear. Additional research is needed to clarify whether soil macropores have important influences on soil physicochemical properties and plant growth in alpine stony soils and to assess their ecological function in maintaining the sustainable development of natural grassland ecosystems. We hypothesized that (1) soil macropore structure differs among the three grassland types on the Qinghai-Tibet Plateau and (2) the differences indirectly affect the growth of vegetation through their effects on soil physical and chemical properties (Leue et al., 2016; Zhang et al., 2017). Therefore, the objective of this study was to quantify the soil macropore features of three types of alpine grasslands using X-ray computed tomography (CT) imaging techniques and provide a better understanding of the interactions between soil properties and plant growth on the northeastern Tibetan Plateau.

MATERIALS AND METHODS

Study Area

This study was performed on the northeastern edge of the Tibetan Plateau in the Tianzhu alpine steppes of Gansu Province, which has a typical continental plateau climate (**Figure 1**). The Tibetan Plateau has a mean elevation of more than 4,000 m, and the high altitude leads to harsh climate conditions, including low temperatures, low moisture levels, high ultraviolet radiation, freeze and thaw cycles and a short growing season. Between 1957 and 2015 in the Jinqiang River watershed, the mean annual temperature was −0.1°C, and the annual mean precipitation was 400 mm. Approximately 70–80% of the annual precipitation occurs from June to September (Wang et al., 2019). Winters are cold and dry, and summers are warm and wet.

To investigate the differences in the features of soil macropores among different grassland types, we selected three typical grassland types in the region: alpine degraded steppe (ADS), alpine typical steppe (ATS) and alpine meadow steppe (AMS) (Sun et al., 2016). The dominant plant species are *Agropyron cristatum* Linnaeus, *Achnatherum splendens* Trin. and *Stipa capillata* Linnaeus in the ADS; *Stipa capillata* Linnaeus, *Artemisia frigida* Willdenow, and *Euphorbia fischeriana* var. *komaroviana* (Prokhanov) in the ATS; and *Potentilla bifurca* Linnaeus, *Kobresia myosuroides* (Villars) Fiori and *Carex moorcroftii* Falconer ex Boott Trans in the AMS. Detailed information can be found in **Table 1**.

Field Vegetation Investigation and Soil Sampling

A soil survey and a sampling campaign were carried out during the active vegetation growth period (July) on the northeastern Tibetan Plateau in 2019. We selected three typical grassland types (ADS, ATS, and AMS) to investigate the vegetation and soil physiochemical properties in forbidden grazing areas. In each

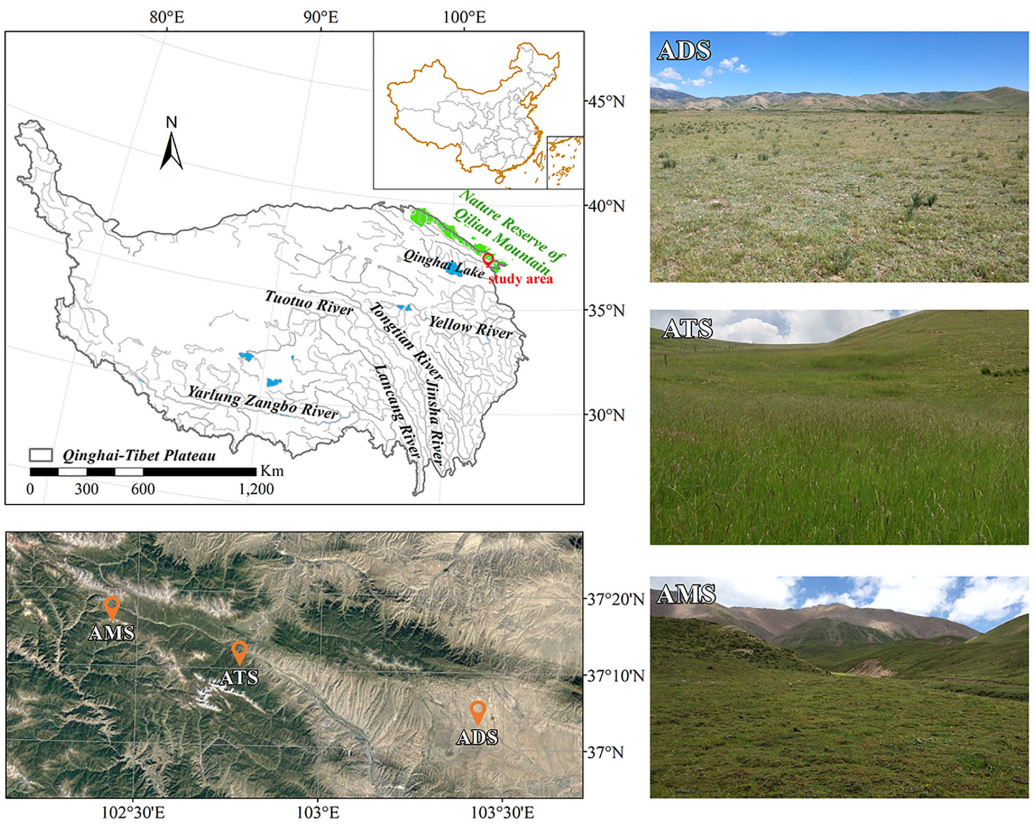

FIGURE 1 | Study area (red circle) and sampling sites (orange unfilled dots). Landscapes of the field sampling sites of alpine degraded steppe (ADS), alpine typical steppe (ATS) and alpine meadow steppe (AMS).

TABLE 1 | Site information for the three grassland types.

Type	Latitude°N	Longitude°E	Elevationm	Soil layercm	Slope position	Slope aspect	Slope°
ADS	37.08	103.43	2675	0–30	Middle	Southeast	4
ATS	37.20	102.78	2858	0–30	Middle	Southeast	6
AMS	37.29	102.43	3641	0–20	Middle	Southeast	10

ADS denotes alpine degraded steppe, ATS denotes alpine typical steppe, and AMS denotes alpine meadow steppe.

grassland type, three small plots (with 50 m between adjacent plots) of 50 cm × 50 cm were set up to investigate the abundance of plant species and calculate the plant diversity (Simpson's index) (Fayiah et al., 2019); then, the aboveground part of each plant was cut off as close to the ground as possible to calculate the aboveground biomass, and the soil under each plot was sampled to determine the belowground biomass in the depth range of 0–30 cm. Next, a standard ring cutter with a volume of 100 cm^3 (50.46 mm in diameter and 50 mm in height) (Yang et al., 2008) was used to collect samples along the soil profile at 0–10, 10–20, and 20–30 cm to calculate the soil bulk density (BD), field water capacity (FC), and soil porosity (SP). At the same position the cutting ring was employed, we used a small shovel to collect approximately 200 g of soil, which was air dried at room temperature and sieved to measure the soil particle composition (clay, silt and sand contents) and soil nutrients [soil organic carbon (SOC), total nitrogen (TN), nitrate nitrogen ($N\text{-}NO_3^-$), ammonium nitrogen ($N\text{-}NH_4^+$), total phosphorus (TP), available phosphorus (AP), total potassium (TK), and available potassium (AK)].

For the collection of undisturbed soil columns for X-ray 3D scanning, we used polyvinyl chloride (PVC) cylinders (3 mm thick walls, diameter 11 cm, length 30 cm) with beveled edges at the bottom to house the soil columns. Before sampling the original soil column, we carefully picked up and moved shrubs and grass from the ground to minimize disturbance. First, each plot was prepared to collect six replicate samples. Because of the high content of rock debris in the soil of the Qilian Mountain area, sampling was difficult and sometimes resulted in the rupture of the PVC cylinders, and the soil column could not be used in the later stage. Ultimately, only three replicates were selected for each grassland type. Because of the high number of rocks in the AMS soil, which was highest among the three grassland types, only 0–20 cm soil columns were obtained. Soil column

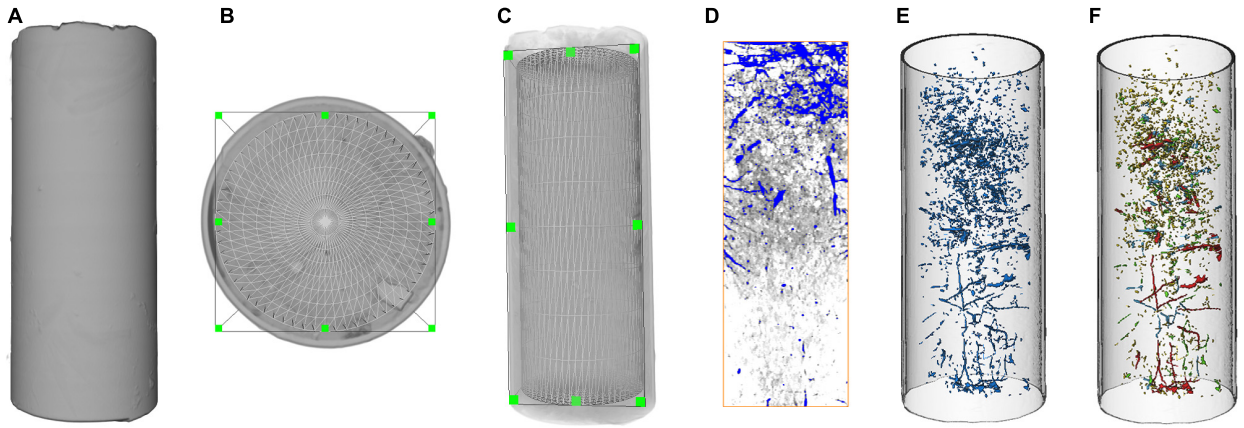

FIGURE 2 | Processing steps of the scanned images of the soil column using Avizo 2019.1 software: 3D imaging of the original soil column **(A)**, top view **(B)** and lateral view **(C)** of ROI (cylinder), cross-section of interactive thresholding segmentation **(D)**, 3D reconstruction of soil macropores **(E)**, and different colors for different sizes of soil macropore surface area **(F)**.

extraction followed the procedure of Sammartino et al. (2012). The soil column was sealed with gauze and plastic film, wrapped in sponge, packed in wheat straw, and transported carefully to avoid compaction and evaporation. We randomly selected three undisturbed soil columns (as replicates) for each grass type and obtained a total of 9 soil column samples for the analysis of soil macropore properties.

Laboratory Analysis

Plant samples and roots were carefully washed, dried in an oven at 65°C for 72 h, and then weighed with an electronic scale. Soil samples used for the determination of soil chemical properties were air dried and passed through a 2 mm sieve. We used the dichromate oxidation method to determine the content of SOC; the micro-Kjeldahl method to determine TN; the alkali diffusion method to determine TP, TK and available nitrogen ($N\text{-}NH_4^+$ and $N\text{-}NO_3^-$); and the sodium bicarbonate ($NaHCO_3$) digestion-Mo-Sb colorimetry method ($NaHCO_3$) to measure AP (Nelson and Sommers, 1982; Jackson, 2005; Bhattacharyya et al., 2006). The soil samples collected with the cutting ring were dried in a 105°C oven for 48 h to a constant weight and used to measure BD, FC, and SP (Zhen et al., 2017).

Quantification of Soil Macropores Using Computed Tomography Scanning

Undisturbed soil columns were scanned by a helical medical CT device (SOMATOM Definition Flash, SIEMENS, Germany) with an excitation voltage of 140 kV at 300 mA at the First Hospital of Lanzhou University. The scanning produced images with 512 pixels × 512 pixels per slice, and the voxel resolution was 0.236 mm × 0.236 mm × 0.6 mm in each reconstructed image. Each column was scanned vertically and generated more than 500 slices, and invalid top and bottom images were removed. Approximately 500 images were used for subsequent analysis.

Avizo 2019.1 (FEI, 2016) software was used for all of the image processing and parameter calculation of the CT images. First, a cylindrical cropping tool was used to obtain the region of interest (ROI): the images were cropped to exclude the area outside the soil column, and all images were carefully examined to identify any soil columns with obvious unnatural macropore morphology caused by the sampling. The edge of each soil column was cut to reduce any possible sampling interference along the edge, and the diameter of each soil column was reduced to 90 mm (**Figures 2B,C**). Second, to improve the image quality, a median filter (radius of 3.0 pixels, a commonly used image-processing method) was used to minimize the noise from all the reconstructed volumes (Hu et al., 2019). Then, a Plexiglas cylinder (0.9 cm in diameter) was inserted into the soil core and removed, its diameter was measured with a digital caliper, and the core was scanned using a helical medical CT device. We assumed an initial threshold to calculate the macropore size when using Avizo 2019.1 software and compared the calculation result with the measured size obtained with a digital caliper. If the difference between the calculated and measured sizes was significant, another threshold was applied to continue the calculation; therefore, the difference was less than 1% (Li et al., 2013; Hu et al., 2016).

After segmentation, the soil macropore networks were reconstructed, and the 3D distribution along the column depth and size distribution [sorted by macropore surface area (SA)] were visualized (**Figure 2**). Since macropores are randomly distributed throughout the soil body, they are sheet-like rather than cylindrical (De Las Cuevas, 1997). The shape of the macropores was irregular and interpreted in three dimensions using Avizo software; therefore, the macropore size was sorted by SA instead of the equivalent radius in this study. According to SA, the macropores were divided into four categories and assigned different colors: $3.14 < SA < 25$ mm^2 (yellow), $25 < SA < 50$ mm^2 (green), $50 < SA < 100$ mm^2 (blue) and $SA > 100$ mm^2 (red). According to Poesen and Lavee (1994), macropores are defined as soil pores with an equivalent radius larger than 0.5 mm, and the SA of a sphere with a radius of 0.5 mm is 3.14 mm^2. Thus, macroporosity (MP) in this study specifically refers to the

volumetric fraction of pores with an SA $\geq$ 3.14 mm^2 (Poesen and Lavee, 1994). In addition, the overall MP, mean number, shape factor (a parameter that describes the shape of an object and equals 1 for a perfect sphere, SF = $SA^3/36\pi V^2$) and volume were calculated using Avizo 2019.1. Typically, macropores are the pathways for the movement of water, air and chemicals in soil. However, the equivalent diameter and shape factor of macropores affect their function, since not all macropores are cylindrical (Poesen and Lavee, 1994; Hillel, 1998).

Statistical Analysis

We analyzed the differences in the number, volume, equivalent radius, SA, shape factor and porosity of soil macropores among the three grassland types using one-way ANOVA followed by multiple comparisons performed using Tukey's *post hoc* test. Differences obtained at a level of $p < 0.05$ were considered significant. To identify the effects of soil macropores on soil physiochemical properties, a principal component analysis (PCA) was conducted to reveal the relations between the distributions of soil physiochemical properties of different grassland types and soil macropore parameters and the contribution of each macropore parameter (Sharifzadeh et al., 2017). The differences in soil physiochemical properties among different grassland types were compared using the one-way ANOVA method as a supplementary method. Finally, a regression analysis was performed to determine the effects of MP and the shape factor on plant communities. We selected a stepwise regression method to reduce the collinearity among the parameters of soil macropores. One-way ANOVA and stepwise regression analysis were performed using SPSS 20.0 software (IBM SPSS version 20, Chicago, IL, United States). PCA and graphing were performed using Canoco 5.0 software, and regression analysis graphs were generated using Origin 2017. As this study is an exploratory study, we here report uncorrected *P* values (Roback and Askins, 2005; Jäschke et al., 2020).

RESULTS

Soil Characteristics of Different Vegetation Types

A variance analysis of the soil properties of the 0–30 cm soil profile at the three sites (ADS, ATS, and AMS) revealed the main differences among the locations (**Table 2**). Soil BD exhibited the order ADS > ATS > AMS, but the difference between ADS and ATS was not significant. The difference in total porosity between ADS and AMS was not significant, and the values in both of these grassland types were higher than that in ATS. The field water holding capacity of AMS was higher than that of ADS and ATS. The contents of SOC and TN differed among the sites ($p < 0.05$, **Table 2**). In addition, the TP content of AMS was much higher than that of ADS and ATS, but there was no significant difference in the distribution of TK in the soil at 20∼30 cm among the sites, whereas the TK contents in the 0∼10 and 10∼20 cm soil layers were much higher in ATS than in ADS and AMS. In terms of the available nutrients, the N-NH_4^+ and N-NO_3 levels in ATS and

TABLE 2 | Physical properties of soil under the three grassland types.

Type	Depth (cm)	Bulk density (g cm^{-3})	Total porosity (cm^{3}cm^{-3})	Field capacity (%)	SOC (g kg^{-1})	TN (g kg^{-1})	N- NH_4^+ (g kg^{-1})	N-NO_3^- (g kg^{-1})	TP (g kg^{-1})	AP (g kg^{-1})	TK (g kg^{-1})	AK (g kg^{-1})
ADS	0–10	1.13 ± 0.02*a*	52.12 ± 5.42*a*	42.18 ± 0.47*a*	22.59 ± 0.87*a*	2.27 ± 0.12*a*	0.0054 ± 0.00*a*	0.0077 ± 0.00*a*	0.59 ± 0.05*a*	0.0015 ± 0.00*a*	5.43 ± 0.15*a*	0.09 ± 0.00*ab*
	10–20	1.11 ± 0.04*a*	55.52 ± 14.53*a*	42.80 ± 6.73*a*	18.51 ± 1.73*a*	2.10 ± 0.17*a*	0.0035 ± 0.00*a*	0.0039 ± 0.00*a*	0.62 ± 0.02*a*	0.0009 ± 0.00*a*	5.57 ± 0.20*ab*	0.08 ± 0.00*a*
	20–30	1.00 ± 0.01*a*	52.87 ± 8.34*a*	52.16 ± 3.30*a*	15.32 ± 2.43*a*	2.00 ± 0.21*a*	0.0022 ± 0.00*a*	0.0041 ± 0.00*a*	0.63 ± 0.03*a*	0.0007 ± 0.00*a*	5.65 ± 0.19*a*	0.08 ± 0.00*a*
	0–30	1.08 ± 0.02*a*	53.50 ± 6.93*a*	45.71 ± 2.86*a*	18.81 ± 2.31*a*	2.12 ± 0.14*a*	0.0037 ± 0.00*a*	0.0234 ± 0.00*a*	0.61 ± 0.03*a*	0.0010 ± 0.00*a*	5.55 ± 0.18*a*	0.08 ± 0.00*a*
ATS	0–10	1.05 ± 0.03*a*	43.09 ± 7.13*b*	47.39 ± 4.81*a*	31.12 ± 0.45*b*	3.43 ± 0.09*b*	0.0074 ± 0.00*a*	0.0129 ± 0.00*b*	0.59 ± 0.01*a*	0.0032 ± 0.0*a*	5.98 ± 0.08*b*	0.10 ± 0.00*a*
	10–20	1.07 ± 0.08*ab*	42.94 ± 9.52*b*	46.60 ± 7.96*a*	22.36 ± 0.64*a*	3.30 ± 0.04*b*	0.0068 ± 0.00*a*	0.0090 ± 0.00*b*	0.55 ± 0.04*a*	0.0022 ± 0.00*a*	5.95 ± 0.11*a*	0.09 ± 0.24*a*
	20–30	1.02 ± 0.06*a*	54.79 ± 2.85*a*	53.56 ± 3.17*a*	16.57 ± 0.48*a*	2.97 ± 0.03*b*	0.0049 ± 0.00*b*	0.0072 ± 0.00*a*	0.49 ± 0.02*b*	0.0012 ± 0.00*a*	5.55 ± 0.12*a*	0.09 ± 0.00*a*
	0–30	1.05 ± 0.03*a*	46.94 ± 7.42*b*	49.18 ± 4.33*a*	23.35 ± 0.47*a*	3.23 ± 0.03*b*	0.0064 ± 0.00*ab*	0.0097 ± 0.00*b*	0.55 ± 0.02*a*	0.0022 ± 0.00*a*	5.83 ± 0.12*a*	0.09 ± 0.00*a*
AM	0–10	0.97 ± 0.09*a*	50.85 ± 2.78*a*	50.54 ± 7.28*a*	69.1 ± 14.52*c*	5.67 ± 0.54*c*	0.0200 ± 0.00*a*	0.0113 ± 0.00*b*	1.46 ± 0.02*b*	0.0159 ± 0.00*b*	5.19 ± 0.14*a*	0.08 ± 0.00*b*
	10–20	0.91 ± 0.06*b*	57.90 ± 4.20*a*	58.28 ± 3.80*b*	53.67 ± 9.15*b*	5.101 ± 0.52*c*	0.0044 ± 0.00*a*	0.0104 ± 0.00*b*	1.44 ± 0.03*b*	0.0071 ± 0.00*b*	5.35 ± 0.06*b*	0.08 ± 0.00*a*
	20–30	0.95 ± 0.09*a*	56.09 ± 6.80*a*	60.49 ± 12.84*b*	38.74 ± 2.51*b*	4.57 ± 0.24*c*	0.0028 ± 0.00*ab*	0.0070 ± 0.00*a*	1.44 ± 0.06*c*	0.0056 ± 0.00*b*	5.48 ± 0.05*a*	0.09 ± 0.00*a*
	0–30	0.94 ± 0.06*b*	54.95 ± 4.31*a*	56.44 ± 3.44*b*	53.85 ± 5.67*b*	5.11 ± 0.39*c*	0.0091 ± 0.00*b*	0.0096 ± 0.00*b*	1.45 ± 0.04*b*	0.0095 ± 0.00*b*	5.34 ± 0.07*a*	0.08 ± 0.00*a*

All data are expressed as the mean ± standard error (SE) of the mean. SOC, soil organic carbon; TN, total nitrogen; TP, total phosphorus; AP, available phosphorus; TK, total potassium; AK, available potassium. Different lowercase letters indicate significant differences among the three grassland types in the same soil layer ($P < 0.05$).

AMS were much higher than those in ADS, and AP in AMS was much higher than that in ADS and ATS. The differences in the distribution of soil AK in the 10∼30 cm layer were not significant.

Macropore Characteristics

The 3D visualizations of the macropore networks in the soils at the ADS, ATS, and AMS sites are shown in **Figure 3**. Overall, the number of macropores in the soil profile gradually increased from ADS to ATS and from ATS to AMS, and the numbers of red and blue macropores increased significantly. The red macropores in the ADS were mainly concentrated at the depth of 10 cm, and the macropores of the other three levels were evenly distributed in the soil profile. The ATS soil had the largest number of blue macropores among the grassland soils, which were evenly distributed throughout the soil profile (**Figure 3**). The AMS soil had the most abundant macropores (925 ± 189), and macropores of all levels were evenly distributed in the AMS soil, in contrast to the distributions in the ADS and ATS soils.

Macropore number was significantly greater in the AMS than in the ADS and ATS, which is consistent with the 3D visualizations of the soil columns. Significant differences in mean macropore volume or equivalent diameter among the three types were not observed (**Table 3**). Without stratification to describe the soil structure, significant differences among the soil types were not observed in mean SA, while at the depth of 0–10 cm, macropore SA was larger in the AMS than in the ADS and ATS, and at 20–30 cm depth, macropore SA was larger in the ATS than in the ADS ($p < 0.05$). The mean shape factor followed the order ADS > ATS > AMS. In contrast, the mean MP followed the order AMS > ATS > ADS ($p < 0.05$) (**Table 3**).

Effects of Macropores on Soil Physicochemical Properties

The results showed that PC1 and PC2 accounted for 83.37% of the explainable variance (**Figure 4**). As shown in **Figure 4**, the contribution of MP was greatest (22.1%), followed by that of the macropore number (18.8%) and shape factor (12.8%).

The PCA results showed that MP was positively correlated with SOC, TN, TP and AP ($p < 0.001$) and that macropore number was significantly correlated with SOC ($p < 0.001$), TN ($p < 0.001$) and AP ($p < 0.05$). Soil BD had significantly negative

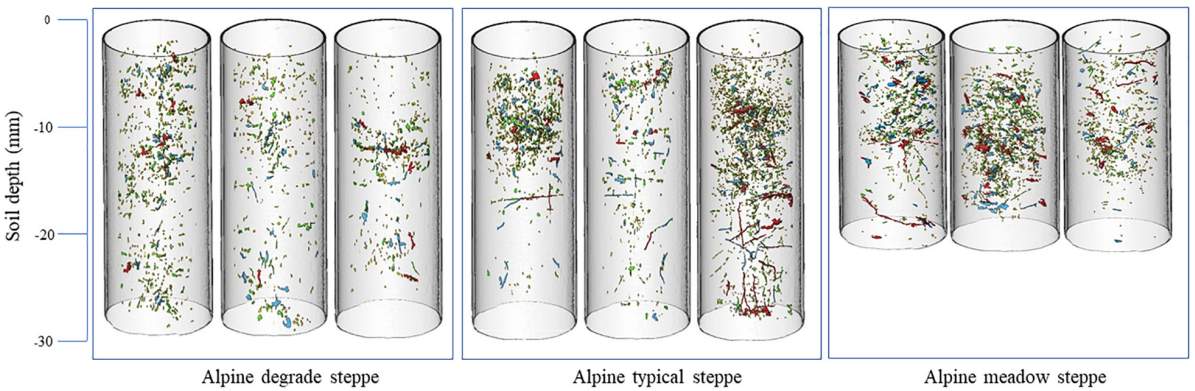

FIGURE 3 | 3D visualization of soil macropore networks in the soil columns of the ADS, ATS and AMS. Yellow represents the surface area (SA) range $0.5 < SA < 25$ mm^2; green represents the range $25 < SA < 50$ mm^2; blue represents the range $50 < SA < 100$ mm^2; and red represents the range $SA > 100$ mm^2.

TABLE 3 | Macropore characteristics under the three grassland types.

Type	Soil layer (cm)	MN	MV (mm^3)	Md_e (mm)	MSA (mm^2)	MSF	MP
ADS	0–10	202 ± 62*a*	4.67 ± 0.26*a*	1.87 ± 0.02*ab*	16.27 ± 0.72*a*	2.20 ± 0.07*a*	0.0018 ± 0.0002*a*
	10–20	201 ± 56*a*	6.57 ± 0.58*a*	1.98 ± 0.03*a*	21.97 ± 1.45*a*	3.06 ± 0.13*a*	0.0024 ± 0.0002*a*
	20–30	134 ± 35*a*	7.63 ± 1.62*a*	1.96 ± 0.04*a*	23.89 ± 3.49*a*	3.02 ± 0.17*a*	0.0015 ± 0.0001*a*
	0–30	537 ± 137*a*	6.12 ± 0.47*a*	1.93 ± 0.02*a*	20.30 ± 1.06*a*	2.73 ± 0.07*a*	0.0019 ± 0.0005*a*
ATS	0–10	541 ± 176*b*	4.50 ± 0.17*a*	1.83 ± 0.02*a*	15.89 ± 0.47*a*	2.19 ± 0.05*a*	0.0051 ± 0.0005*b*
	10–20	363 ± 65*a*	5.52 ± 0.32*a*	1.90 ± 0.02*b*	19.14 ± 0.91*a*	2.51 ± 0.09*b*	0.0039 ± 0.0005*b*
	20–30	116 ± 67*a*	21.03 ± 8.51*b*	2.14 ± 0.08*b*	54.41 ± 18.69*b*	4.46 ± 0.85*a*	0.0015 ± 0.0002*a*
	0–30	1020 ± 100*b*	6.75 ± 0.98*a*	1.89 ± 0.01*a*	21.43 ± 2.37*a*	2.56 ± 0.11*a*	0.0035 ± 0.0010*b*
AMS	0–10	531 ± 82*b*	6.74 ± 0.74*b*	1.90 ± 0.02*b*	20.59 ± 1.54*b*	2.26 ± 0.08*a*	0.0050 ± 0.0005*b*
	10–20	394 ± 135*a*	6.36 ± 0.44*a*	1.91 ± 0.02*b*	20.96 ± 1.14*a*	2.45 ± 0.08*b*	0.0044 ± 0.0009*b*
	0–20	925 ± 189*b*	6.58 ± 0.46*a*	1.90 ± 0.02*a*	20.75 ± 1.01*a*	2.34 ± 0.06*b*	0.0047 ± 0.0014*b*

All data are expressed as the mean ± standard error (SE) of the mean. MN, mean number; MSA, mean surface area of all macropores; MSF, mean shape factor; MV, mean macropore volume; Mde, mean equivalent diameter; MP, mean macroporosity. Different lowercase letters within a column indicate significant differences among the three grassland types in the same soil layer ($P < 0.05$).

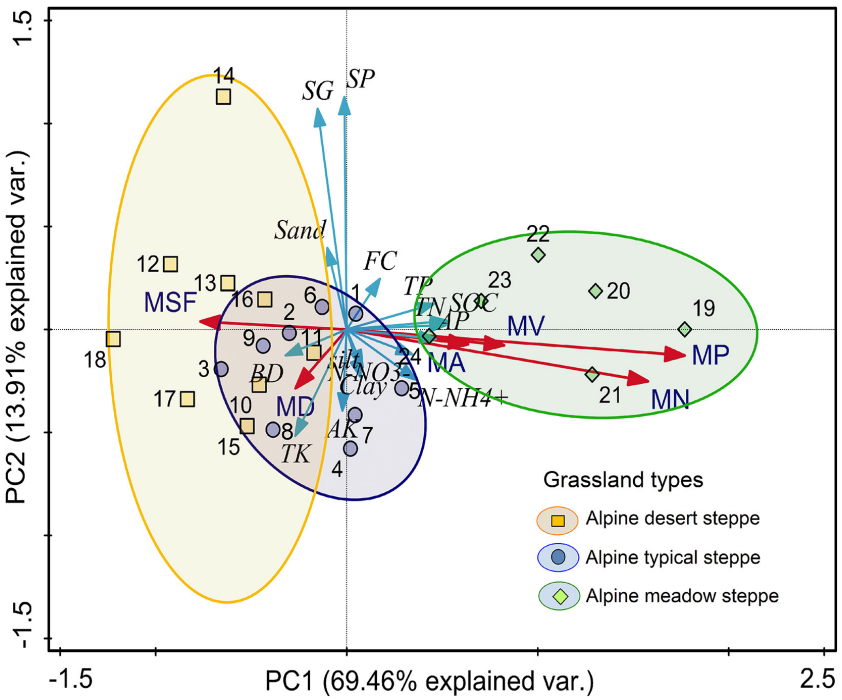

FIGURE 4 | Results of PCA showing the relationships between soil macropore characteristics and soil physiochemical properties. The red arrow indicates macropore characteristics (MV, macropore volume; MA, macropore area; MSF, macropore shape factor; MN, macropore number; MP, macroporosity), and the blue arrow indicates soil physiochemical properties (SOC, soil organic carbon; SP, soil porosity; SG, specific gravity; BD, bulk density; FC, field capacity; TN, total nitrogen; TP, total phosphorus; AP, available phosphorus; TK, total potassium).

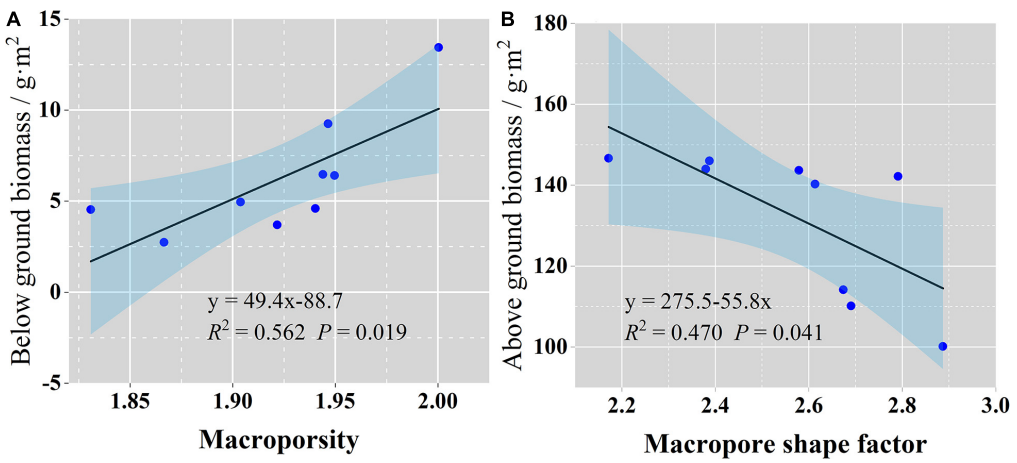

FIGURE 5 | Relationships between belowground biomass **(A)**, aboveground biomass and soil macropore characteristics **(B)**. Black lines indicate regression fitting lines; the light blue shadowed area indicates the 95% confidence interval of regression.

relationships with macropore SA, volume and the shape factor ($p < 0.05$, **Figure 4**).

Relationships Between Macropores and Plant Growth

Stepwise regression reduced the collinearity among the soil macropore parameters such that only MP was input into the model. The regression analysis revealed that the macropores had a great impact on the belowground biomass of the three types of grassland communities (**Figure 5A**, $R^2 = 0.562$, $p < 0.05$). Similarly, only one parameter, the macropore shape factor, was entered into the model of aboveground biomass, and it was shown to affect the aboveground biomass of each grassland type community (**Figure 5B**, $R^2 = 0.47$, $p < 0.05$). However, none of the macropore parameters were

input into the model of vegetation diversity of the three grassland types.

DISCUSSION

Alpine steppe soil contains many rock fragments; thus, quantifying macropores via traditional methods leads to inaccuracies, overestimating or underestimating the effects of macropores on soil properties and vegetation growth (Bauke et al., 2017; Ilek et al., 2019). Using X-ray CT technology, soil macropores can be visualized and quantified in undisturbed soil columns. The results of the 3D visualization of the soil macropore network showed that the soil MP in the AMS was larger than that in the ATS and that the macropore content was smallest in the ADS (**Figure 3** and **Table 3**), which may be related to the location of the northeastern Tibetan Plateau in an arid area of northern China and the limited precipitation received by degraded grasslands. The ADS is located in the arid and semiarid region of northern China and has a lower altitude than the other two steppe regions, which leads to lower activity levels of soil animals (e.g., earthworms) and plant roots that promote the formation of macropores in this region than in typical grasslands and alpine meadows. Generally, low macropore contents are observed in degraded grasslands (Hu et al., 2020). Kravchenko et al. (2015) proposed a feedback process in which more pores lead to stronger microbial activity, which promotes soil animal and plant activities and leads to the production of more pores (Meurer et al., 2020). In the 3D visualization, the ADS soil had almost no tubular or highly continuous large pores, while the other two grassland types exhibited many pores of this type (**Figure 3**); the pattern in ADS soil was caused by the reduced activities of soil animals and plant roots. This finding is consistent with the work of Luo et al. (2010), who demonstrated that highly continuous, tubular soil macropores are formed by earthworm activity and root decay. Hu et al. (2020) reached a similar conclusion in their study of typical meadow soil types on the Tibetan Plateau.

Although significant differences in macropore volume, equivalent diameter and SA in the 0–30 cm soil profile were not observed among the three steppes, macropore volume, equivalent diameter and surface area in the 0–10 cm surface soil were significantly larger in the AMS than in the ATS and ADS (**Table 3**), which may be related to the mostly cold-tolerant plant species with well-developed root systems that occur in the AMS. The main roots and coarse roots of meadow plant species are mainly distributed in the topsoil (Hu et al., 2019). The soil moisture contents of the ADS and ATS are low, and most of the plant roots have to extend to great soil depths to absorb water and nutrients (Cai and Shen, 2002; Wu et al., 2011; Zhang et al., 2017). Hu et al. (2019) used X-ray tomography to study the relationship between the root system and macropores in undisturbed soil under different shrubs in northern China and found that the soil MP and mean macropore volume showed significant positive correlations with the root network.

The PCA results showed that the first two principal components explained 69.46% of the variation in soil physical and chemical properties, of which soil MP accounted for approximately one-third, at 22.1%. These findings suggest that the soil macropore structure can determine the soil physicochemical properties to large extents. The correlation analysis results also showed that soil MP had significant positive correlations with the SOC, TN, AP and TP contents (**Figure 4**), which may be related to the large amounts of organic coatings attached to the soil pore wall in structural soil (Gerke et al., 2012; Leue et al., 2016). These findings are consistent with the results of Zhang et al. (2017), who reported that soil macropores increase soil aeration, which enhances the microbial activity in the macropores, the decomposition of dead animal and root litter, and the release of organic matter (Luo et al., 2010). Previous studies have shown that soil macropores can be regarded as biogeochemical hotspots because the biopores formed by biological activities (earthworm and root activities) are rich in various microorganisms, and the aeration of macropores accelerates the turnover rate of nutrients, such as N and P, and thus increases the supply of soil and plant root nutrients (Bundt et al., 2001; Kuzyakov and Blagodatskaya, 2015).

The effects of soil macropores on nutrient contents impact plant growth (Passioura, 1991). Our results showed that among the studied factors, the macropore shape factor had the greatest impact on the aboveground biomass of the three grasslands. As the macropore shape factor increased, the aboveground biomass declined (**Figure 5A**), which may have been related to the more irregular shape and poorer connectivity of macropores with a larger shape factor. Under such conditions, plant roots cannot easily extend into the soil, which leads to insufficient nutrients and water for plant growth and a decline in aboveground biomass. Similarly, the belowground biomass increased with soil MP, indicating that the soil macropores provide enough space for root organisms to obtain nutrients and water. Previous studies suggest that an increase in MP allows more P to be transported from the surface soil to the root systems for root system construction and that the presence of macropores leads to a higher growth rate of the root system (Athmann et al., 2013; Gaiser et al., 2013; Han et al., 2015).

CONCLUSION

In this study, the characteristics of soil macropores in three alpine grasslands in the northeastern Tibetan Plateau were visualized and quantitatively analyzed using the X-ray CT technique. The results showed that the macropores were significantly different among the three grasslands and that the vertical distribution of macropores in the soil profile also differed among the different types of grassland soil. The AMS soil had more macropores than the other soil types, and the relatively increased macropore content in the AMS promoted the turnover of soil nutrients; thus, the AMS aboveground biomass was higher than that of the other two steppes. However, the impact of macropores on biodiversity in the three grasslands (Simpson's index) was not statistically significant. We conclude that macropores in alpine stony soils can increase soil nutrients, improve soil conditions, and provide space for plant root growth, thereby promoting

plant biomass. However, this promotion effect does not vary with plant species. These findings deepen our understanding of the effects of soil macropores on the physiochemical properties of soil and plant growth in alpine stony soils and provide a theoretical basis for maintaining the sustainable development of natural grassland ecosystems.

DATA AVAILABILITY STATEMENT

The raw data supporting the conclusions of this article will be made available by the authors, without undue reservation.

AUTHOR CONTRIBUTIONS

YZ: conceptualization, methodology, investigation, and writing – original draft. NC: review and editing. C-kZ and X-xD: analyzed the data and draw figures. C-mZ: reviewing and editing, and supervision. All authors contributed to the article and approved the submitted version.

FUNDING

This work was supported by the National Key Research and Development Program of China (2019YFC0507401), Strategic Priority Research Program of the Chinese Academy of Sciences (XDA20100101), and the National Natural Science Foundation of China (NSFC) (Grant No. 31901364).

ACKNOWLEDGMENTS

We are grateful to the two reviewers and the handling editor YJ for providing insightful comments and suggestions.

REFERENCES

Athmann, M., Kautz, T., Pude, R., and Köpke, U. (2013). Root growth in biopores-evaluation with in situ endoscopy. *Plant Soil* 371, 179–190. doi: 10.1007/s11104-013-1673-5

Bauke, S. L., Landl, M., Koch, M., Hofmann, D., Nagel, K. A., Siebers, N., et al. (2017). Macropore effects on phosphorus acquisition by wheat roots–a rhizotron study. *Plant Soil* 416, 67–82. doi: 10.1007/s11104-017-3194-0

Beven, K., and Germann, P. (2013). Macropores and water flow in soils revisited. *Water Resour.* 52, 218–242.

Bhattacharyya, R., Prakash, V., Kundu, S., Ghosh, B. N., Srivastva, A. K., and Gupta, H. S. (2006). Potassium balance as influenced by farmyard manure application under continuous soybean-wheat cropping system in a Typic Haplaquept. *Geoderma* 137, 155–160. doi: 10.1016/j.geoderma.2006.08.006

Bronick, C. J., and Lal, R. (2005). Soil structure and management: a review. *Geoderma* 124, 3–22.

Bundt, M., Jäggi, M., Blaser, P., Siegwolf, R. T. W., and Hagedorn, F. (2001). Carbon and nitrogen dynamics in preferential flow paths and matrix of a forest soil. *Soil Sci. Soc. Am. J.* 65, 1529–1538. doi: 10.2136/sssaj2001.6551529x

Cai, K. Z., and Shen, H. (2002). Root: dynamic interface of plant and soil – introduce for the sixth international roots research conference. *Acta Ecol. Sin.* 22, 139–140. (in Chinese),

Colombi, T., Braun, S., Keller, T., and Walter, A. (2017). Artificial macropores attract crop roots and enhance plant productivity on compacted soils. *Sci. Total Environ.* 574, 1283–1293. doi: 10.1016/j.scitotenv.2016.07.194

De Las Cuevas, C. (1997). Pore structure characterization in rock salt. *Eng. Geol.* 47, 17–30. doi: 10.1016/s0013-7952(96)00116-0

Fayiah, M., Dong, S., Li, Y., Xu, Y., Gao, X., Li, S., et al. (2019). The relationships between plant diversity, plant cover, plant biomass and soil fertility vary with grassland type on Qinghai-Tibetan Plateau. *Agric. Ecosyst. Environ.* 286:106659. doi: 10.1016/j.agee.2019.106659

FEI (2016). *Amira & Avizo 3D Software*. Available online at: https://www.fei.com/software/amira-avizo/ (accessed March 1, 2017).

Fuhrmann, I., Maarastawi, S., Neumann, J., Amelung, W., Frindte, K., Knief, C., et al. (2019). Preferential flow pathways in paddy rice soils as hot spots for nutrient cycling. *Geoderma* 337, 594–606. doi: 10.1016/j.geoderma.2018.10.011

Gaiser, T., Perkons, U., Küpper, P. M., Kautz, T., Uteau-Puschmann, D., Ewert, F., et al. (2013). Modeling biopore effects on root growth and biomass production on soils with pronounced sub-soil clay accumulation. *Ecol. Model.* 256, 6–15. doi: 10.1016/j.ecolmodel.2013.02.016

Gao, Z., Hu, X., Li, X. Y., and Li, Z. C. (2020). Effects of freeze-thaw cycles on soil macropores and its implications on formation of hummocks in alpine meadows in the Qinghai Lake watershed, northeastern Qinghai-Tibet Plateau. *J. Soils Sediments* 21, 245–256. doi: 10.1007/s11368-020-02765-2

Gerke, K. M., Skvortsova, E. B., and Korost, D. V. (2012). Tomographic method of studying soil pore space: current perspectives and results for some Russian soils. *Eurasian Soil Sc.* 45, 700–709. doi: 10.1134/s1064229312070034

Guimarães, R. M., Lamandé, M., Munkholm, L. J., Ball, B. C., and Keller, T. (2017). Opportunities and future directions for visual soil evaluation methods in soil structure research. *Soil Till. Res.* 173, 104–113. doi: 10.1016/j.still.2017.01.016

Hamblin, A. P., and Hamblin, J. (1985). Root characteristics of some temperate legume species and varieties on deep, free-draining entisols. *Austr. J. Agric. Res.* 36, 63–72. doi: 10.1071/ar9850063

Han, E., Kautz, T., Perkons, U., Uteau, D., Peth, S., Huang, N., et al. (2015). Root growth dynamics inside and outside of soil biopores as affected by crop sequence determined with the profile wall method. *Biol. Fert. Soils* 51, 847–856. doi: 10.1007/s00374-015-1032-1

Hillel, D. (1998). *Environmental Soil Physics: Fundamentals, Applications, and Environmental Considerations*. Waltham, MA: Academic Press.

Hlaváčiková, H., Holko, L., Danko, M., and Novák, V. (2019). Estimation of macropore flow characteristics in stony soils of a small mountain catchment. *J. Hydrol.* 574, 1176–1187. doi: 10.1016/j.jhydrol.2019.05.009

Hodge, A., Berta, G., Doussan, C., Merchan, F., and Crespi, M. (2009). Plant root growth, architecture and function. *Plant Soil* 321, 153–187. doi: 10.1007/s11104-009-9929-9

Hu, X., Li, X. Y., Li, Z. C., Gao, Z., Wu, X. C., Wang, P., et al. (2020). Linking 3D soil macropores and root architecture to near saturated hydraulic conductivity of typical meadow soil types in the Qinghai Lake Watershed, northeastern Qinghai-Tibet Plateau. *Catena* 185:104287.

Hu, X., Li, X. Y., Wang, P., Liu, Y., Wu, X. C., Li, Z. C., et al. (2019). Influence of exclosure on CT-measured soil macropores and root architecture in a shrub-encroached grassland in northern China. *Soil Till. Res.* 187, 21–30.

Hu, X., Li, Z. C., Li, X. Y., and Liu, L. Y. (2016). Quantification of soil macropores under alpine vegetation using computed tomography in the Qinghai Lake Watershed, NE Qinghai–Tibet Plateau. *Geoderma* 264, 244–251. doi: 10.1016/j.geoderma.2015.11.001

Ilek, A., Kucza, J., and Witek, W. (2019). Using undisturbed soil samples to study how rock fragments and soil macropores affect the hydraulic conductivity of forest stony soils: some methodological aspects. *J. Hydrol.* 570, 132–140. doi: 10.1016/j.jhydrol.2018.12.067

Iversen, B. V., Lamandé, M., Torp, S. B., Greve, M. H., Heckrath, G., dejonge, L. W., et al. (2012). Macropores and macropore transport: relating basic soil properties to macropore density and soil hydraulic properties. *Soil Sci.* 177, 535–542. doi: 10.1097/ss.0b013e31826dd155

Jackson, M. L. (2005). *Soil Chemical Analysis: Advanced Course*. Madison, WI: UW-Madison Libraries Parallel Press.

Jarvis, N. J. (2007). A review of non-equilibrium water flow and solute transport in soil macropores: principles, controlling factors and consequences for water quality. *Eur. J. Soil Sci.* 58, 523–546. doi: 10.1111/j.1365-2389.2007.00915.x

Jarvis, N. J., Koestel, J., and Larsbo, M. (2016). Understanding preferential flow in the vadose zone: recent advances and future prospects. *Vadose Zone J.* 15, 1–11. doi: 10.2136/vzj2015.05.0079

Jäschke, Y., Heberling, G., and Wesche, K. (2020). Environmental controls override grazing effects on plant functional traits in Tibetan rangelands. *Funct. Ecol.* 34, 747–760. doi: 10.1111/1365-2435.13492

Kautz, T., Amelung, W., Ewert, F., Gaiser, T., Horn, R., Jahn, R., et al. (2013). Nutrient acquisition from arable subsoils in temperate climates: a review. *Soil Biol. Biochem.* 57, 1003–1022. doi: 10.1016/j.soilbio.2012.09.014

Kautz, T., Lüsebrink, M., Pätzold, S., Vetterlein, D., Pude, R., Athmann, M., et al. (2014). Contribution of anecic earthworms to biopore formation during cultivation of perennial ley crops. *Pedobiologia* 57, 47–52. doi: 10.1016/j.pedobi.2013.09.008

Kravchenko, A. N., Negassa, W. C., Guber, A. K., and Rivers, M. L. (2015). Protection of soil carbon within macro-aggregates depends on intra-aggregate pore characteristics. *Sci. Rep.* 5:16261.

Kuka, K., Illerhaus, B., Fox, C. A., and Joschko, M. (2013). X-ray computed microtomography for the study of the soil-root relationship in grassland soils. *Vadose Zone J.* 12, 1–10.

Kuzyakov, Y., and Blagodatskaya, E. (2015). Microbial hotspots and hot moments in soil: concept & review. *Soil Biol. Biochem.* 83, 184–199. doi: 10.1016/j.soilbio.2015.01.025

Landl, M., Huber, K., Schnepf, A., Vanderborght, J., Javaux, M., Bengough, A. G., et al. (2017). A new model for root growth in soil with macropores. *Plant Soil* 415, 99–116. doi: 10.1007/s11104-016-3144-2

Leue, M., Eckhardt, K. U., Ellerbrock, R. H., Gerke, H. H., and Leinweber, P. (2016). Analyzing organic matter composition at intact biopore and crack surfaces by combining DRIFT spectroscopy and pyrolysis-field ionization mass spectrometry. *J. Plant Nutr. Soil Sc.* 179, 5–17. doi: 10.1002/jpln.201400620

Li, X. Y., Hu, X., Zhang, Z. H., Peng, H. Y., Zhang, S. Y., Li, G. Y., et al. (2013). Shrub hydropedology: preferential water availability to deep soil layer. *Vadose Zone J.* 12, 1539–1663.

Luo, L., Lin, H., and Li, S. (2010). Quantification of 3D soil macropore networks in different soil types and land uses using computed tomography. *J. Hydrol.* 393, 53–64. doi: 10.1016/j.jhydrol.2010.03.031

Maier, F., van Meerveld, I., Greinwald, K., Gebauer, T., and Lustenberger, F. (2020). Effects of soil and vegetation development on surface hydrological properties of moraines in the Swiss Alps. *Catena* 187:104353. doi: 10.1016/j.catena.2019.104353

Meurer, K., Barron, J., Chenu, C., Coucheney, E., Fielding, M., Hallett, P., et al. (2020). A framework for modelling soil structure dynamics induced by biological activity. *Glob. Change Biol.* 26, 5382–5403. doi: 10.1111/gcb.15289

Nelson, D. W., and Sommers, L. (1982). "Total carbon, organic carbon, and organic matter," in *Methods of Soil Analysis. Part 2. Chemical and Microbiological Properties*, ed. A. L. Page (Madison, WI: American Society of Agronomy), 539–579.

Passioura, J. B. (1991). Soil structure and plant growth. *Soil Res.* 29, 717–728. doi: 10.1071/sr9910717

Pierret, A., Capowiez, Y., Belzunces, L., and Moran, C. J. (2002). 3D reconstruction and quantification of macropores using X-ray computed tomography and image analysis. *Geoderma* 106, 247–271. doi: 10.1016/s0016-7061(01)00127-6

Poesen, J., and Lavee, H. (1994). Rock fragments in top soils: significance and processes. *Catena* 23, 1–28. doi: 10.1016/0341-8162(94)90050-7

Qin, Y., Yi, S., Chen, J., Ren, S., and Ding, Y. (2015). Effects of gravel on soil and vegetation properties of alpine grassland on the Qinghai-Tibetan plateau. *Ecol. Eng.* 74, 351–355. doi: 10.1016/j.ecoleng.2014.10.008

Rabot, E., Wiesmeier, M., Schlüter, S., and Vogel, H. J. (2018). Soil structure as an indicator of soil functions: a review. *Geoderma* 314, 122–137. doi: 10.1016/j.geoderma.2017.11.009

Roback, P. J., and Askins, R. A. (2005). Judicious use of multiple hypothesis tests. *Conserv. Biol.* 19, 261–267. doi: 10.1111/j.1523-1739.2005.00269.x

Sammartino, S., Michel, E., and Capowiez, Y. (2012). A novel method to visualize and characterize preferential flow in undisturbed soil cores by using multislice helical CT. *Vadose Zone J.* 11:vzj2011.0100.

Sharifzadeh, S., Ghodsi, A., Clemmensen, L. H., and Ersbøll, B. K. (2017). Sparse supervised principal component analysis (SSPCA) for dimension reduction and variable selection. *Eng. Appl. Artif. Intel.* 65, 168–177. doi: 10.1016/j.engappai.2017.07.004

Sun, J., Qin, X., and Yang, J. (2016). The response of vegetation dynamics of the different alpine grassland types to temperature and precipitation on the Tibetan Plateau. *Environ. Monitor. Assess.* 188:20.

Wang, D. B., Wang, X. Y., Wu, Y., and Lin, H. L. (2019). Grazing buffers the effect of climate change on the species diversity of seedlings in an alpine meadow on the Tibetan Plateau. *Ecol. Evol.* 9, 1119–1126. doi: 10.1002/ece3.4799

Wang, W., Kravchenko, A. N., Smucker, A. J. M., and Rivers, M. L. (2011). Comparison of image segmentation methods in simulated 2D and 3D microtomographic images of soil aggregates. *Geoderma* 162, 231–241. doi: 10.1016/j.geoderma.2011.01.006

Wu, Z. T., Dijkstra, P., Koch, G. W., Peñuelas, J., and Hungate, B. A. (2011). Responses of terrestrial ecosystems to temperature and precipitation change: a meta-analysis of experimental manipulation. *Glob. Change Biol.* 17, 927–942. doi: 10.1111/j.1365-2486.2010.02302.x

Xu, G., Chao, Z., Wang, S., Hu, Y., Zhang, Z., Duan, J., et al. (2010). Temperature sensitivity of nutrient release from dung along elevation gradient on the Qinghai-Tibetan plateau. *Nutr. Cycl. Agroecosys.* 87, 49–57. doi: 10.1007/s10705-009-9311-6

Yang, Y., Fang, J., Tang, Y., Ji, C., Zheng, C., He, J., et al. (2008). Storage, patterns and controls of soil organic carbon in the Tibetan grasslands. *Glob. Change Biol.* 14, 1592–1599. doi: 10.1111/j.1365-2486.2008.01591.x

Zhang, Y., Niu, J., Zhang, M., Xiao, Z., and Zhu, W. (2017). Interaction between plant roots and soil water flow in response to preferential flow paths in northern China. *Land Degrad. Dev.* 28, 648–663. doi: 10.1002/ldr.2592

Zhen, Q., Ma, W., Li, M., He, H., Zhang, X., and Wang, Y. (2017). Reprint of "Effects of vegetation and physicochemical properties on solute transport in reclaimed soil at an opencast coal mine site on the Loess Plateau, China". *Catena* 148, 17–25. doi: 10.1016/j.catena.2016.09.012

Zwartendijk, B. W., Van Meerveld, H. J., Ghimire, C. P., Bruijnzeel, L. A., Ravelona, M., and Jones, J. P. G. (2017). Rebuilding soil hydrological functioning after swidden agriculture in eastern Madagascar. *Agric. Ecosyst. Environ.* 239, 101–111. doi: 10.1016/j.agee.2017.01.002

Conflict of Interest: The authors declare that the research was conducted in the absence of any commercial or financial relationships that could be construed as a potential conflict of interest.

Publisher's Note: All claims expressed in this article are solely those of the authors and do not necessarily represent those of their affiliated organizations, or those of the publisher, the editors and the reviewers. Any product that may be evaluated in this article, or claim that may be made by its manufacturer, is not guaranteed or endorsed by the publisher.